COULOMB BARRIER TOTAL SCREENING BY BOSE-EINSTEIN-CONDENSED DEUTERIUM IN PALLADIUM BLISTERS AND REACTION CHAINS IN HIGH-DENSITY HYSTERESIS

NUCLEAR REACTIONS IN SOLIDS

KEYWORDS: *inside-defects BEC, barrier quantum screening, reaction chains*

FRANCESCO PREMUDA*
Facoltà di Ingegneria dell'Università degli Studi di Bologna, Laboratorio di Ingegneria Nucleare di Montecuccolino, via dei Colli n. 16, 40136 Bologna, Italy

Received July 23, 1993
Accepted for Publication July 22, 1997

Downloaded by [Australian Catholic University] at 05:53 21 September 2017

A theoretical model is proposed in order to explain, via ordinary physics, fundamental aspects of the cold fusion phenomena experimentally observed. These phenomena include unexpected high fusion reaction rates at low temperatures, the paradox of low neutron emission compared to the energy release observed, the cold fusion dependence on critical temperature, neutronic stimulation, and the constitution of nuclei with high electric charge. This theory is based on the hypothesis that a degenerate, cold $D_1^{2+}e^-$ plasma may be created inside lattice defects through a sudden deuteron discharge from a saturated metal lattice. The proposed method is based on the perturbative solution of Vlasov-Poisson kinetic-electric equations. A Fourier transformation of such equations proves that the plasma behaves like an ideal Bose gas of electronically screened deuterons. This approach shows that a high particle density can exist with no pressure increase above the limiting value reached at Bose-Einstein condensation (BEC) and that the electrical repulsion field between positive ions disappears below the critical temperature for BEC. Inside the voids created by defects, the behavior of the cold degenerate plasma below critical temperature suppresses the Coulomb barrier between any pair of ions, in particular those that will fuse. The absence of Coulomb barrier allows one to simply predict fusion reaction rates of the order of those found experimentally and the particle trapping in high-density condensate causing fusion chains. The main reactions involved are D_1^2-T_1^3 and D_1^2-He_2^3. Subsequent fusions of the main reaction products lead to nuclei of greater complexity. A high neutron multiplication factor via deuteron disintegrations is calculated. Neutron bursts, temperature, and pressure excursions are also predicted. Finally, new procedures for inducing such reactions outside metal lattices are suggested.

I. INTRODUCTION

In a number of cold fusion experiments,[1–3] unexpected results were observed, such as the paradox of low neutron emission compared to the number of fusions needed to generate the released energy, together with the unexpectedly high fusion reaction rates rising with the temperature decrease.

One[4] of the first theoretical explanations for these experimental paradoxes was a phenomenological hypothesis proposing the existence of small zones having a high density of deuterium to explain energy and tritium generation in terms of fusion chains.[5,6] However, the high-density hypothesis itself and the high fusion reaction rates still demanded a fundamental interpretation.

At the same time other authors suggested that the anomalously high fusion reaction rates were due to a plasma made of deuterons and conduction electrons inside the metal lattice. This approach focuses on electron screening of the Coulomb repulsion between deuterons[7] or on a coherent fusion mechanism[8,9] for a deuteron with all those belonging to a coherence plasma domain inside the lattice.

More recently, some research groups have proposed to consider screening improvement by electrons at discontinuity surfaces,[10–12] such as grain surfaces, interfaces between different metals, or between air and metal.

*E-mail: francesco.premuda@mail.ing.unibo.it

Downloaded by [Australian Catholic University] at 05:53 21 September 2017

However, despite reports in Refs. 13, 14, and 15, and discussion in the scientific community on the attractive pseudoforces due to bosonic affinity, prior studies seem to have completely ignored the quantum mechanical implications of Coulomb barrier screening in cold nuclear fusion (CNF) phenomena occurring at the temperature and density conditions typical of strongly degenerate plasmas in solids.

While Coulomb barrier suppression and asymptotic freedom are very important,[9] these issues are not satisfactorily resolved by many authors. The proposed superradiance theory for CNF, which explicitly violates "asymptotic freedom,"[16] is also difficult to accept as is admitting the possibility that a whole domain of deuterons, localized in the lattice sites, could interact coherently with a somewhat localized surplus deuteron. For this to happen, the deuteron has to overcome the barriers preventing its free motion inside the lattice.[17] Only the delocalization of deuterons, such as that occurring inside a Bose-Einstein-condensed plasma in a lattice defect, could allow free coherent fusion.

The heuristic idea of high densities (10^3 to 10^4 times solid density) explains[4–6] the few neutron paradox and high fusion reaction rates between many freely neighboring deuterium-deuterium (D-D) couples avoiding the introduction of exotic D-D fusion laws. In this framework a theory for CNF inside defects, where deuterons of a Bose-Einstein-condensed (BEC) phase are completely delocalized, appears more "natural" than CNF models in lattices or at lattice surfaces. This does not necessarily exclude the other two classes of models: Surface CNF effects should in any case be taken into account separately; future studies could further develop also in defects a partially coherent–partially incoherent fusion model, though inside strongly degenerate BEC plasma, the high density seems to restrict the coherence domains in favor of incoherent fusion. The BEC of $D_1^{2+}e^-$ plasma inside defects represents the main evolution of the present work with respect to previous contributions.[4-6]

The present approach, by predicting CNF inside $D_1^{2+}e^-$ BEC plasma within defects, explains Coulomb barrier suppression and thus explains how all well-established nuclear physics laws are acting in fusion freely with respect to Coulomb barrier and to any other nonnuclear physical reality. In this way, the proposed model remains completely in the domain of "ordinary physics," leaving the explanation of the low neutron emission and of the discrepancy between fusion reaction and tritium accumulation rates to the mechanism of fusion chains inside BEC deuterium plasma spots.

Independently of the preceding considerations, a density of the order of 10^3 to 10^4 times solid densities, like those reached in inertial confinement fusion reactors, appears difficult to reach inside the metal lattice. In fact, CNF phenomena were observed in various metals[18–20] with no strict correlation to the characteristics of the particular lattice structure. However, according to the assumptions at the basis of the proposed model, the class of possible CNF deuterium plasma-metal systems is not so wide ranging because it must exhibit the following:

1. high deuterium absorption capability
2. good ionizing properties
3. capability to generate sufficiently high pressures without destroying the lattice, i.e., to act as an efficient ionic pump
4. appropriate working temperature range (in order to allow BEC)
5. capability to have large defects or suitable containment cells (where the deuterium plasma could undergo BEC with improved superconductivity and Coulomb barrier suppression).

For a metal lattice with such characteristics, a deuterium plasma is created inside defects via a two-step process.[21,22] First, a high loading level x (>0.8) of D_1^{2+} per Pd atom is reached in the Pd lattice generating a positive potential distribution[9] due to deuterium plasma internal to the lattice. This plasma is highly unstable in itself and for the inclusion of additional deuterons, so a sudden discharge of D_1^{2+} ions, followed by electrons, occurs to create a cold degenerate $D_1^{2+}e^-$ plasma under high pressures in the lattice blisters. This pressure condition represents the main difference between the foundations of the present theory and the Liboff[23,24] hypotheses for CNF in a degenerate plasma at a temperature near absolute zero in the external void.

Much higher temperatures with respect to the Liboff conditions ($\simeq$300 K rather than a few kelvins) are possible for BEC at the high pressures generated by the discharge from the metal to the blisters.

As a matter of fact, Liboff,[23,24] on the basis of a variational technique proposed by Lee and Feenberg,[25] predicted an electron screening at temperatures near absolute zero and at low pressures, allowing a deuteron wave-function superposition, which favors nuclear fusion significantly in a sort of liquid deuterium metal state. However, the Hansen-Mazighi[26] work, based on a different variational approach, invalidated the wave-function overlap predicted by Liboff, thus leaving Liboff's theory open to question.

On the other hand both the Hansen-Mazighi[26] and the Liboff[23,24] models describe the plasma as constituted by charged bosons in a constant, i.e., static, neutralizing background. The present work proposes a dynamic model involving both bosonic and fermionic plasma components to solve the open question about a possible large particle-particle overlap within the BEC limit. The adopted method consists in a perturbative solution of the Poisson-Vlasov system, which describes the actual long-wave hydrodynamic fluctuations of the plasma. Since these fluctuations were not included in variational calculations of Refs. 26 or 23 and 24, more sophisticated effects of dynamic

Downloaded by [Australian Catholic University] at 05:53 21 September 2017

screening of both electrons and bosons in even more general conditions can now be incorporated.

In fact, a study of a $D_1^{2+}e^-$ degenerate plasma under high pressures (up to 10^5 to 10^7 bar) and at temperatures starting from $\simeq$300 K is considered from a quantum mechanical transport point of view. Such an approach leads step by step to the conclusion that deuterons, screened by electrons, induce the degenerate plasma to behave as an ideal Bose gas undergoing BEC. This conclusion implies the absence over short time intervals of the macroscopic Pd blistering effect typically found after light hydrogen loading and can explain the superconductivity phenomena in deuterated Pd. In addition the high deuterium density reached locally during BEC in the system, which causes particle trapping and consequently fusion chains with gamma- and X-ray damping, is also accounted for. Finally, the most fundamental aspect of cold fusion—the practical disappearance of the Coulomb barrier—is justified both mathematically and physically via BEC of deuterons; the resulting high reaction rates increase as $D_1^2e^-$ plasma temperature decreases and reach the maximum values when the deuterium plasma temperature T becomes less than the critical $T_c \sim n^{2/3}$ for deuteron BEC. Due to such density dependence, T_c starts at 0 before the deuterium loading and then reaches $T \simeq T_0 = 300$ K, finally achieving values of thousands of kelvins, as the deuterium loading of the blisters proceeds. This "density hysteresis" allows sufficiently long times for energy generation via fusion reactions before a final Bose-Einstein decondensation, possible only for T greater than the final T_c value.

The model proposed not only provides a valid mechanism for Coulomb barrier suppression, satisfying completely asymptotic freedom requirements for nuclear fusions without barrier, but also coherently explains the following phenomena:

1. disagreement between energy, neutron, and tritium rates of emission from CNF systems, in whose dense zones the particles generated by fusion are trapped
2. temperature dependence of CNF phenomena due to the existence of BEC critical temperatures
3. need for high x values to cause BEC in defects
4. possible generation of high-Z ions in no-barrier fusion reactions, involving any ion in the plasma with deuterium
5. occurrence of CNF in various metals
6. possibility of CNF stimulation through extra-neutron injection
7. key role of the concentration of T_1^3 in determining the success of CNF experiments,[27] weakly active with detritiated heavy water
8. higher critical temperature for superconductivity of D-loaded palladium and less blistering when the lattice is loaded with D instead of H
9. lattice damage observed after fusions and the CNF efficiency of the load-unload (high-low current) mechanism adopted by Takahashi[28] as improving BEC. With this mechanism the deuterium saturation process at high current, leading to instability of $x \simeq 1$ and then to download of deuterium into defects, is induced without apparent lattice damage any time the current rises; this happens because repeated lattice saturations, induced through current injection, increase the BEC zones both in size and number. Note that the initial absence of lattice damage is observed only with deuterium loading, whereas cracks are observed from the beginning with light hydrogen loading. For this reason the proposed model cannot be considered a fracto-fusion model.

As an explanation of both neutron bursts and continuous neutron and energy emissions with tritium creation on the basis of a local protonic fusion chain in a single BEC zone of a blister or of simultaneous local proton and collective neutron chains in a blister lattice inside the metal (the latter corresponding to the highest energy production and to the lowest neutron escape probability from the whole system), the proposed model appears to apply to all Preparata-type CNF systems[9] and can also partially explain gas-discharge experiments.[29]

Its validity is tied to CNF phenomena involving a deuterium background; however, experiments involving predominantly light hydrogen background are explained by an extension of this theory now in progress.

II. VLASOV PERTURBED EQUATIONS FOR BOSONS AND FERMIONS INSIDE A COLD $D_1^{2+}e^-$ DEGENERATE PLASMA LOCATED IN LATTICE DEFECTS

According to Refs. 21 and 22, the saturation of a Pd lattice with deuterium first induces a sudden discharge of D_1^{2+} ions, followed by conduction electrons, inside lattice voids such as blisters or rifts, either preexisting or created by the discharge itself. The consequent rapid rise of pressure inside such defects creates density conditions where neighboring atomic potential wells exhibit strongly lowered thresholds with respect to a dilute atom system[30] with a consistent decrease of ionization potential, vanishing as the density assumes Mott density value.[31] At that point, the high discharge rate precludes a consistent recombination, thus allowing constitution of a $D_1^{2+}e^-$ cold degenerate plasma. To treat its electrical behavior and deduce an extended Debye length for such a plasma, a classical approach[32] based on combined Vlasov and Poisson equations has been adopted. In fact, in view of such neutral plasma properties near equilibrium, the collisional aspects entering the Boltzmann-Uehling-Uhlenbeck (BUU) equation,[33] generalizing the Boltzmann equation in the quantum mechanical sense, are taken into account by simply assuming that the equilibrium distributions, to which

Downloaded by [Australian Catholic University] at 05:53 21 September 2017

electron and deuteron distributions will rapidly approach with time after a perturbation, are those of Fermi-Dirac and Bose-Einstein statistics related to the vanishing properties of BUU collisional operators.[34,35]

Let us introduce now in our neutral $D_1^{2+}e^-$ plasma, at equilibrium with temperature $T = T_0 \leq 300$ K, the perturbation constituted by an ion I^+ of +Ne positive charge traveling with v_0 velocity. The collisional term in BUU operates in approximate proportion to the difference $F^\pm - F_0^\pm$ between the actual and equilibrium distributions through the inverse of the greatest of its time constants. As they are all very short with respect to the mean, between collisions, time λ/v_0 for the slow v_0 in which we are interested (limit of $v_0 \to 0$) in view of CNF phenomena, then the positive and negative ions of our plasma satisfy, respectively, Vlasov equations

$$\frac{DF^\pm(\boldsymbol{x},\boldsymbol{v},t)}{Dt} \pm \frac{e}{m^\pm}\boldsymbol{\epsilon}\cdot\frac{DF^\pm(\boldsymbol{x},\boldsymbol{v},t)}{D\boldsymbol{v}} = 0 \tag{1}$$

with $m^+ = m_0^*$ and $m^- = m_e^*$ being effective masses of deuterons and electrons,

$$\frac{D}{Dt} \equiv \frac{\partial}{\partial t} + \boldsymbol{v}\cdot\frac{\partial}{\partial \boldsymbol{x}} \ , \tag{2}$$

substantial time-derivative and $\bar{\boldsymbol{\epsilon}}$ electric field satisfying Poisson's equation

$$\boldsymbol{\nabla}\cdot\boldsymbol{\epsilon} = 4\pi\rho \ . \tag{3}$$

The perturbative approach adopted then implies that

$$F^\pm = F_0^\pm + \epsilon g^\pm$$

and

$$\boldsymbol{\epsilon} = 0 + \epsilon \boldsymbol{E} \ , \tag{4}$$

where the Fermi-Dirac distribution can be assumed for F_0^-, then

$$F_0^-(E)\,dE = \frac{1}{e^{(E-E_F)/T}+1}\,dE \tag{5a}$$

with Fermi energy

$$E_F = \left(\frac{3}{8\pi}\right)^{2/3}\frac{h^2}{2m^-}\,n_0^{2/3} \ , \tag{5b}$$

n_0 being the common value of D_1^{2+} and e^- equilibrium densities.

When looking at an overestimation of screening length, the influence of deuterons can be disregarded because they should in any case increase the efficiency of the screening of the Coulomb interaction between deuterons or between the I^+ ion and any deuteron D_1^{2+}. (See Refs. 14 and 15 for attractive pseudoforces created by a repulsive screening.) Consequently the calculation of λ, reduced to that of λ_F Fermi screening length, which replaces in this instance λ_D Debye length, could then be restricted to take into account $g^- \neq 0$ only, when proving that our plasma is a degenerate "ideal" plasma and finding on this basis the character of F_0^+, equilibrium D_1^{2+} boson distribution, in order to go back finally, with a known F_0^+, to a complete treatment of the problem taking into account both $g^\pm \neq 0$. For brevity, a complete solution is offered from the beginning for non-vanishing g^- and g^+ equations. The F_0^+ is left to be determined later in line with the conclusions about λ_F Fermi screening length.

Via substitution of expression (4) inside Vlasov equation (1) and Poisson equation (3) and appropriate linearization, the equation

$$\frac{\partial g^\pm}{\partial t} + \boldsymbol{v}\cdot\frac{\partial g^\pm}{\partial \boldsymbol{x}} \pm \frac{e}{m^\pm}\boldsymbol{E}\cdot\frac{\partial F_0^\pm}{\partial \boldsymbol{v}} = 0 \tag{6}$$

is obtained, as the equilibrium distributions $F_0^\pm$ solve Vlasov equation (1) for $\boldsymbol{\epsilon} = 0$ in a plasma optically as wide as ours due to the high n_0 reached in the lattice discharge, and

$$\boldsymbol{\nabla}\cdot\boldsymbol{E} = 4\pi(\rho_s + \rho_p^+ + \rho_p^-) \ , \tag{7a}$$

provided ρ_s and $\rho_p^\pm$ are defined as

$$\rho_s = Ne\delta(\boldsymbol{x} - \boldsymbol{v}_0 t)$$

and

$$\rho_p^\pm = \pm e\int g^\pm\,d\boldsymbol{v} \ . \tag{7b}$$

Once introduced, the Fourier transforms via

$$g^\pm(\boldsymbol{x},\boldsymbol{v},t) = \frac{1}{(2\pi)^4}\int d\boldsymbol{k}\int d\omega\,\tilde{g}^\pm(\omega,\boldsymbol{k},\boldsymbol{v})e^{i(\boldsymbol{k}\cdot\boldsymbol{x}-\omega t)} \tag{8a}$$

and

$$\boldsymbol{E}(\boldsymbol{x},t) = \frac{1}{(2\pi)^4}\int d\boldsymbol{k}\int d\omega\,\tilde{E}(\omega,\boldsymbol{k})e^{i(\boldsymbol{k}\cdot\boldsymbol{x}-\omega t)} \ , \tag{8b}$$

representing $g^\pm$ and $\boldsymbol{E}$ expanded into planar waves, Vlasov equations lead to

$$\tilde{g}^\pm = \mp\frac{ien_0}{m^\pm}\,\frac{\tilde{E}}{\omega - \boldsymbol{k}\cdot\boldsymbol{v}}\cdot\frac{\partial f_0^\pm}{\partial \boldsymbol{v}} \ , \tag{9a}$$

when letting $f_0^\pm = 1/n_0 F_0^\pm$. The Fourier transform of Eq. (7a) further yields

$$i\boldsymbol{k}\cdot\tilde{E} = 4\pi(\tilde{\rho}_s + \tilde{\rho}_p^+ + \tilde{\rho}_p^-) \tag{9b}$$

with

$$\tilde{\rho}_s = 2\pi Ne\delta(\omega - \boldsymbol{k}\cdot\boldsymbol{v}_0)$$

and

$$\tilde{\rho}_p^{\pm} = \pm e \int \tilde{g}^{\pm}\, d\boldsymbol{v} \ , \tag{9c}$$

to be then coupled with Eq. (9a).

III. DIELECTRIC CONSTANT AND SCREENING FOR $D_1^{2+}e^-$ DEGENERATE COLD PLASMA

The consideration of longitudinal waves, i.e., of the component $[(\boldsymbol{k}\cdot\tilde{E})/k^2]\boldsymbol{k}$ of $\tilde{E}$ only, leads, after combining Eqs. (9), to the solution

$$i\boldsymbol{k}\cdot\tilde{E} = \frac{4\pi\tilde{\rho}_s(\boldsymbol{k},\omega)}{\epsilon(\boldsymbol{k},\omega)} \ , \tag{10}$$

with

$$\epsilon(\boldsymbol{k},\omega) = \epsilon(k,\omega) = 1 + \frac{\omega_{p^+}^2}{k^2}\int \frac{\boldsymbol{k}\cdot\dfrac{\partial f_0^+}{\partial \boldsymbol{y}}}{\omega - \boldsymbol{k}\cdot\boldsymbol{v}}\, d\boldsymbol{v} + \frac{\omega_{p^-}^2}{k^2}\int \frac{\boldsymbol{k}\cdot\dfrac{\partial f_0^-}{\partial \boldsymbol{v}}}{\omega - \boldsymbol{k}\cdot\boldsymbol{v}}\, d\boldsymbol{v} \tag{11}$$

and

$$\omega_{p^{\pm}}^2 = \frac{4\pi n_0 e^2}{m^{\pm}} \ , \tag{11a}$$

for the transformed electric field induced by the ion I^+ of charge $+Ne$ traveling with velocity v_0 in our cold degenerate $D_1^{2+}e^-$ plasma at temperature $T \le T_0 = 300$ K. The quantity $\epsilon(k,\omega)$ represents the dynamic dielectric response function of the plasma to the perturbation; thus, the corresponding time- and position-dependent electric field will be, via Eq. (8b), written again for longitudinal waves only as

$$\boldsymbol{E}(\boldsymbol{x},t) = \frac{1}{(2\pi)^4}\int d\boldsymbol{k}\int d\omega\, e^{i(\boldsymbol{k}\cdot\boldsymbol{x}-\omega t)}\,\frac{\boldsymbol{k}\cdot\tilde{E}}{k^2}\,\boldsymbol{k} = \frac{-2ieN}{(2\pi)^2}\int d\boldsymbol{k}\,\frac{e^{i\boldsymbol{k}(\boldsymbol{x}-\boldsymbol{v}_0 t)}\boldsymbol{k}}{k^2\epsilon(k,\boldsymbol{k}\cdot\boldsymbol{v}_0)} \ . \tag{12}$$

The static special case of Eq. (11), of course valid also for $v_0 \cong 0$, is

$$\epsilon(k,0) = 1 + \frac{\omega_{p^+}^2}{k^2}h^+ + \frac{\omega_{p^-}^2}{k^2}h^- \tag{13a}$$

with

$$h^{\pm} = -\int \frac{\boldsymbol{k}\cdot\dfrac{\partial f_0^{\pm}}{\partial \boldsymbol{v}}}{\boldsymbol{k}\cdot\boldsymbol{v}}\, d\boldsymbol{v} \tag{13b}$$

that suitable elaborations reduce to the form

$$h^{\pm} = -\frac{2\pi(2m^{\pm})^{5/2}}{h^3}\int E^{1/2}\,\frac{\partial f_0^{\pm}}{\partial E}\, dE \ . \tag{14}$$

Temporarily neglecting the contribution to $\epsilon(\kappa,0)$ of the positive ions by roughly setting $h^+ = 0$, as could be appropriate in the usual heavy ion metal lattice, for our low-temperature degenerate cold plasma, the unique nonvanishing h is approximately

$$h^- \cong \frac{2\pi(2m^-)^{5/2}}{h^3}\,\frac{1}{n_0}\int_0^{\infty} E^{1/2}\delta(E - E_F)\, dE = \frac{3}{4}(2m^-)\,\frac{1}{E_F} \tag{15}$$

so that the static dielectric constant is

$$\epsilon(k,0) = 1 + \left(\frac{k_F}{k}\right)^2 \ , \tag{16a}$$

where

$$k_F^2 = \omega_{p^-}^2 h^- = \frac{6\pi n_0 e^2}{E_F} \ . \tag{16b}$$

Thus in the static case, expression (12) for the electric field becomes

$$\boldsymbol{E}(\boldsymbol{x}) = \frac{-2Ne}{(2\pi)^2}\int d\boldsymbol{k}\,\frac{i\boldsymbol{k}e^{i\boldsymbol{k}\cdot\boldsymbol{x}}}{k^2 + k_F^2} \ . \tag{17}$$

A comparison of Eq. (17) with

$$\boldsymbol{E}(\boldsymbol{x}) = -\nabla\phi(\boldsymbol{x}) = -\frac{1}{(2\pi)^3}\int i\boldsymbol{k}\tilde{\phi}(\boldsymbol{k})e^{i\boldsymbol{k}\cdot\boldsymbol{x}}\, d\boldsymbol{k} \ , \tag{18}$$

introducing the electrical potential, shows that

$$\tilde{\phi}(\boldsymbol{k}) = \tilde{\phi}(k) = \frac{4\pi Ne}{k^2 + k_F^2} \tag{19}$$

and hence that

$$\phi(r) = \frac{Nee^{-k_F r}}{r} \tag{20}$$

Downloaded by [Australian Catholic University] at 05:53 21 September 2017

Downloaded by [Australian Catholic University] at 05:53 21 September 2017

represents the screened potential created by I^+ at rest in the plasma. For the degenerate cold plasma with a degenerate electronic component now under consideration, the distance

$$\lambda_F = \frac{1}{k_F} = \left(\frac{E_F}{6\pi n_0 e^2}\right)^{1/2} \tag{21a}$$

will replace the classical Debye length

$$\lambda_D = \left(\frac{T}{4\pi n_0 e^2}\right)^{1/2} . \tag{21b}$$

The aforedetermined Fermi length λ_F results independent of temperature and less affected than λ_D by density variations, as can be seen from

$$\lambda_F = \left(\frac{E_F}{6\pi n_0 e^2}\right)^{1/2} = \left(\frac{3}{8\pi}\right)^{1/3} \frac{h}{(12\pi m^- e^2)^{1/2}} \frac{1}{n_0^{1/6}} . \tag{22}$$

According to Rosenbluth and Sagdeev[36] the "ideality parameter" $n_0\lambda^3$ assumes for $\lambda = \lambda_D$ the expression

$$n_0\lambda^3 = \left(\frac{T}{4\pi e^2}\right)^{3/2} \frac{1}{n_0^{1/2}} \tag{23a}$$

and for $\lambda = \lambda_F$ the form

$$n_0\lambda^3 = \frac{3}{8\pi} \frac{h^3}{(12\pi m^- e^2)^{3/2}} n_0^{1/2} . \tag{23b}$$

This means that for a classical hot plasma the ideality decreases with decreasing T and increasing n_0, whereas for a degenerate cold plasma the ideality for sufficiently low T values remains instead unchanged when T decreases and increases for increasing n_0.

Thus, for sufficiently high pressures, a cold degenerate $D_1^{2+}e^-$ plasma is expected to be sufficiently ideal, at least in the sense that, on the average, kinetic energy will predominate over potential energy. In addition, when the problem was faced from another point of view,[37] λ in the case of a degenerate plasma appeared reduced by electron screening at least to the order of magnitude of a Bohr radius, the potential $\phi(r)$ satisfying the Thomas-Fermi equation for the atomic potential. The conclusion is that the deuteron gas component of our plasma behaves like an ideal Bose gas in the conditions considered—low temperatures, $T = T_0 \leq 300$ K, and densities much higher than solid densities (see white dwarf conditions in the Rosenbluth-Sagdeev[36] introductory diagram for plasma classification).

IV. THE IDEAL BOSE GAS OF SCREENED DEUTERONS

The conclusion that the set of deuterons in our degenerate cold plasma $D_1^{2+}e^-$ behaves like an ideal Bose gas is strictly connected with the idea that there is no spin correlation between the screening free-electron background and any single screened deuteron.

As is well known, for an ideal Bose gas the boson energy distribution is

$$F_0^+(E)\,dE = \frac{1}{e^{\frac{E-\mu}{T}} - 1} dE \quad \text{for } \mu < 0 , \quad \text{i.e., } T > T_c , \tag{24a}$$

where μ represents the chemical potential.

The critical temperature for BEC is

$$T_c = \frac{h^2}{\pi\left[\zeta\left(\frac{3}{2}\right)\right]^{2/3} 2m^+} n_0^{2/3} , \tag{24b}$$

in which ζ represents the Riemann Z function. After Pd saturation, the deuteron discharge from the metal lattice increases plasma density n_0 inside defects from 0 to $n_0 = n_{0_c}$, at which the corresponding critical temperature T_c, expressed in Eq. (24b), equals the fixed laboratory temperature $T = T_0$. At this point BEC begins as μ vanishes inside Eq. (24a), where an $(n_0 - n_{0_c})\delta(E)$ term should be added[35] to obtain BUU solutions taking into account that some deuterons go to occupy the fundamental quantum state characterized by $\boldsymbol{p} = 0$ ($E = 0$). Additional N deuterons being discharged increase n_0, leaving the F_0^+ expression [Eq. (24a)] invariant as N additional deuterons in turn occupy the fundamental $\boldsymbol{p} = 0$ state, so that, according to the well-known equation of state

$$P = \left(\frac{2\pi m^+}{h^2}\right)^{3/2} \zeta\left(\frac{5}{2}\right) T^{5/2} \qquad T < T_c , \tag{25}$$

pressure P will no longer increase with deuteron discharges during BEC because the additional deuterons in the $E = 0$ state cannot transmit any impulse.

According to Eq. (25) the plasma pressure for $T \cong T_0 = 300$ K reaches a value, constant during the discharge, of 1.5×10^5 bar lower than $P_B = 10^7$ bar required to have blistering or rifts generated inside a Pd lattice. This fact explains why loading Pd with D_1^{2+} ions does not cause blistering in the first days of a CNF cell's operation, when fusions have not yet started to release a significant amount of energy. This is in contrast to the continuous pressure increase, up to P_B or higher, during an H_1^1 loading of Pd lattice and successive discharge into defects.

On the contrary, after $T_c \cong T_0 = 300$ K is reached and $T_c > T = T_0$ are also attained, in agreement with Eq. (24b) during initial Pd load with deuterium and discharge, then Eq. (25) ensures that for D_1^{2+} ions, $P = P(T_0)$ will be the maximum pressure during the process. Thus, once the BEC

Downloaded by [Australian Catholic University] at 05:53 21 September 2017

begins, very high n_0 values can be reached without plasma resistance because the plasma cannot oppose further deuteron load increasing the pressure. This possibility of very high n_0 values not only leads the system to occupy the region of "degenerate ideal plasma," typical of white dwarfs in the plasma classification diagram,[36] but also allows neutrons and charged particles to be trapped inside the degenerate cold plasma itself; these are the conditions for fusion chains with low neutron emission, provided of course that high fusion reaction rates can be reached, as shown in Sec. VII, for both D-D and deuterium-tritium (D-T) fusions (and many other collateral fusion reactions including D-He and D-H fusions too). In Secs. V and VI it will be proved that short-distance Coulomb repulsion among deuterons does not constitute the limiting factor for n_0 values but is rather the energy released by fusions, beginning for $T < T_c$, that prevents n_0 to reach the nuclear density level, $\sim 10^{15}$ times solid density.

In fact a sort of thermodynamic hysteresis may be expected for the Bose-Einstein-condensed plasma. The initial value T_0 assumed by plasma temperature T can take any value smaller than 300 K to make easier, according to Eq. (24b), the achievement of $T_c = T = T_0$. As n_0 increases because of the injection of D_1^{2+} and e^- at a constant rate and temperature T, due to Eq. (24b), T_c increases with $n_0^{2/3}$, being a pure expression of plasma degeneracy.

When the critical parameters take the values $T_c = T$ and $P_c = P$, the BEC process starts, and any further injection of D_1^{2+} at a constant T increases n_0 and T_c, and in turn the fraction $[1 - (T/T_c)^{3/2}]$ of Bose-Einstein-condensed D_1^{2+} at $\bar{p} = 0$. Finally, such a high maximum $T_c = T_{MC}$ will be reached that a rise of T to the laboratory temperature or even higher, due to energy released by fusion, could not lead the system to verify the decondensation condition $T > T_c$ for a sufficiently long time, allowing increases of $p(T)$ up to possible final microexplosions, with macroscopic blistering effects, before fusions stop when T exceeds T_{MC}.

V. VLASOV PERTURBED EQUATIONS WITH A CONTRIBUTION FROM BOSON MOBILITY AND ACCURATE STATIC DIELECTRIC CONSTANT FOR $D_1^{2+}e^-$ COLD DEGENERATE PLASMA

The scope of this section is to reconsider the assumption for h^+ made in Sec. III and then solve Eqs. (12), (13), and (14), having at our disposal the results of Secs. III and IV for a better evaluation of $h^{\pm}$, both now considered as nonvanishing. Once assumption (24a) is justified for the screened deuterons, a much more accurate evaluation of dielectric static constant $\epsilon(k,0)$ becomes possible with an appropriate calculation of $h^{\pm}$ via Eqs. (14) + (5a) + (24a). On this basis for $T > T_c$ and so for $\mu < 0$,

$$\epsilon(k,0) = 1 + \frac{8\pi^2 e^2}{h^3 k^2} \times \left\{ (2m^+)^{3/2} \int_0^\infty dE \frac{1}{E^{1/2}\left[e^{\frac{E-\mu}{T}} - 1 \right]} + (2m^-)^{3/2} \int_0^\infty dE \frac{1}{E^{1/2}\left[e^{\frac{E-E_F}{T}} + 1 \right]} \right\} . \tag{26}$$

What is essential for an understanding of the physical behavior of the cold degenerate plasma considered is that, while the "fermionic contribution integral"

$$\int_0^\infty dE \frac{1}{E^{1/2}\left[e^{\frac{E-E_F}{T}} + 1 \right]} \tag{27}$$

always remains convergent and finite for any T and even for $T \to 0$, the "bosonic contribution integral"

$$\int_0^\infty dE \frac{1}{E^{1/2}\left[e^{\frac{E-\mu}{T}} - 1 \right]} , \tag{28}$$

though convergent for $\mu < 0$ goes to $+\infty$ for $T \to T_c +$ and so $\mu \to 0-$.

VI. COLD DEGENERATE $D_1^{2+}e^-$ PLASMA BOSE-EINSTEIN-CONDENSED AS A SUPERMETAL

The divergence of the dielectric constant $\epsilon(k,0)$ as $T \to T_c$ means that once the degenerate plasma $D_1^{2+}e^-$ is Bose-Einstein-condensed, no more electric fields can be established through the introduction of a positive ion at rest or slowly moving within the partially condensed system of deuterons.

The deep physical reason of the divergence of $\epsilon(k,0)$ in deuterium plasma for $T \le T_c$ will be discussed for $N = 1$, although Sec. V considerations hold even for $N > 1$ (as for He_2^{3+}). Before an ion of charge e (e.g., H_1^{1+}, D_1^{2+}, T_1^{3+}) is introduced in the original neutral $D_1^{2+}e^-$ plasma, the field $\boldsymbol{E} = 0$ exists everywhere, as a sum of both vanishing fields created by the electronically screened deuterons of the excited phase and by the delocalized condensed phase $\boldsymbol{p} = 0$ deuterons, spread in a medium wide in terms of λ_F's. After the introduction of a perturbative ion, the plasma can be schematically represented as one where the additional ion (H_1^{1+}, D_1^{2+}, T_1^{3+}) replaced a deuteron D_1^{2+} of the previous distribution. Without BEC this original deuteron with the remaining deuterons of the original plasma should cause a perturbed deuteron distribution with density n_p oscillating with respect to the original equilibrium distribution n_0. However, BEC for $n_p > n_0$ and

Downloaded by [Australian Catholic University] at 05:53 21 September 2017

Bose-Einstein decondensation for $n_p < n_0$ will lead to an electronically screened excited deuteron distribution of the previous shape, creating, together with the additional positive ion substituting for the previous deuteron, a zero electrical field. The excess deuteron remains, mixed with the electron bath, in a delocalized state with $\boldsymbol{p} = 0$ without contributing to the electric field, because a homogeneous system of screened deuterons in BEC is practically infinite in terms of λ units and consequently is symmetric around any internal position. As a result, the vanishing field conditions are reached with $\epsilon(k,0) = +\infty$ only for $T \leq T_c$, whatever the singly ionized positive ion introduced is, thus allowing Coulomb barrier annihilation not only for D-D but also for D-T and D-H fusions and others. Of course, a partial effect of field balancing through BEC can also occur for $T > T_c$ to the extent that the perturbed deuteron distribution can lead, in special positions, to deuteron densities such that locally the increased T_c exceeds T.

In addition, Coulomb barrier annihilation occurs analogously for D-He_2^3 and D-He_2^4 fusions and for many other fusion reactions, thus leading to the generation of high-Z nuclei, which have been detected experimentally.

This system could be called a "supermetal" because not only electrons, as in metals, but also positive ions can freely move in it to balance perturbative fields perfectly for $T \leq T_c$.

VII. COLD FUSION REACTION RATES IN $D_1^{2+}e^-$ BOSE-EINSTEIN-CONDENSED PLASMA

An accurate treatment of dynamic effects in $\epsilon(k, \boldsymbol{k}\cdot\boldsymbol{v}_0)$ on the Coulomb barrier between fast-moving deuterons when collisional aspects causing BEC have insufficient time to act and an accurate treatment for the nonvanishing Coulomb barrier effects for temperatures $T > T_c$ for BEC are left to future investigations. The present analysis is confined to the effects of the static $\epsilon(k,0)$ divergence and of the corresponding static Coulomb barrier annihilation for $T \leq T_c$, on the couple of nuclei going to fuse. Fusion reaction rates between A and B nuclei classically represented as

$$RR_{FF} = \int_{R_3} d\boldsymbol{v}_\mathrm{A} \int_{R_3} d\boldsymbol{v}_\mathrm{B} f^\mathrm{A}(\boldsymbol{v}_\mathrm{A}) f^\mathrm{B}(\boldsymbol{v}_\mathrm{B}) |\boldsymbol{v}_\mathrm{A} - \boldsymbol{v}_\mathrm{B}| \sigma_F(|\boldsymbol{v}_\mathrm{A} - \boldsymbol{v}_\mathrm{B}|) \tag{29}$$

will assume an especially simple form for cold fusion in a Bose-Einstein-condensed plasma ($T \leq T_c$). In such conditions f^A and f^B are Fermi-Dirac or Bose-Einstein statistics distributions with an additional $\delta(E)$ term.[34,35] Since the Coulomb barrier when $T \leq T_c$ is practically eliminated for slow-moving ions, the contribution to RR_{FF} of interacting low-energy particles will strongly predominate, giving special importance to the fusion cross-section behavior for $|\boldsymbol{v}_\mathrm{A} - \boldsymbol{v}_\mathrm{B}| \to 0$. Simple quantum mechanical considerations[38] lead to Fermi's second golden rule and so to

$$|\boldsymbol{v}_\mathrm{A} - \boldsymbol{v}_\mathrm{B}| \cdot \sigma_\mathrm{F}(|\boldsymbol{v}_\mathrm{A} - \boldsymbol{v}_\mathrm{B}|) = \frac{1}{\pi\hbar^4} \langle |\mathcal{H}_{if}|^2 \rangle \frac{P^2_{\mathrm{A'B'}}}{|\boldsymbol{v}_{\mathrm{A'}} - \boldsymbol{v}_{\mathrm{B'}}|} \ , \tag{30}$$

where

$$\langle |\mathcal{H}_{if}|^2 \rangle = \Omega^2 \langle |H_{if}|^2 \rangle = \Omega^2 \left| \int \Psi_f^* U \Psi_i \, d\tau \right|^2 \tag{31}$$

and U is the nuclear interaction energy acting only at a short distance. This implies a dependence of $\mathcal{H}_{if}$ from the superposition of wave functions in a nuclear volume, whereas Ω represents the volume occupied by the system (now the defect volume) on which the wave functions are normalized. There is thus no reason, from a quantic point of view, to discriminate between excited and condensed deuterons—in any case ψ_i and ψ_f represent delocalized plane waves—in view of the aforementioned superposition on the nuclear volume.

The absence of the Coulomb barrier at low temperatures $T \leq T_c$ causes the exponential tunneling factors not to appear in $\langle |\mathcal{H}_{if}| \rangle^2$. *The* $\mathcal{H}_{if}$ matrix will be also independent[38] of $|\boldsymbol{v}_\mathrm{A} - \boldsymbol{v}_\mathrm{B}|$ due to the exothermic character of fusion reactions. Since the remaining part of the right side of Eq. (30) also exhibits the same property for the identical reasons, the conclusion is that approximately

$$|\boldsymbol{v}_\mathrm{A} - \boldsymbol{v}_\mathrm{B}| \sigma_\mathrm{F}(|\boldsymbol{v}_\mathrm{A} - \boldsymbol{v}_\mathrm{B}|) = \gamma_\mathrm{AB} = \text{const.} \ , \tag{32}$$

leaving a more detailed and accurate treatment to future studies.

The normalization of $f^\mathrm{A}(\boldsymbol{v}_\mathrm{A})$ and $f^\mathrm{B}(\boldsymbol{v}_\mathrm{B})$ to n_0^A and n_0^B then leads to

$$RR_{FF}^\mathrm{AB} = \gamma_\mathrm{AB} n_0^\mathrm{A} n_0^\mathrm{B} \quad \text{for } T \leq T_c \ , \tag{33}$$

whereas the Coulomb barrier effects should appear and strongly attenuate reaction rates for $T > T_c$. In this last condition the RR_{FF}^AB can be temporarily approximated to a zero value, leaving a study of the effects on RR_{FF}^AB of the gradual reappearance of the Coulomb barrier to future investigations.

Note that at this point, either n_0^A or n_0^B, or both, can equal n_0 of $D_1^{2+}e^-$ plasma and that $T_c \sim n_0^{2/3}$.

Thus for sufficiently high n_0 , T_c will be even greater than the plasma temperature $T = T_0 = 300$ K, and the reaction rates RR_{FF}^AB will be proportional to n_0 and n_0^B ($= n_0^\mathrm{D} = n_0$ or n^T, n^H, n^He). Despite that in principle no upper limit exists for these densities other than nuclear matter density (10^{15} times solid density), the real physical densities are self-limiting due to power density generation by fusion. In fact for $T_c > T$, an increase in density n_0 will cause an increase in reaction rates RR_{FF} and associated energy generation, increasing T, which can result locally in a final Bose-Einstein decondensation of

Downloaded by [Australian Catholic University] at 05:53 21 September 2017

the plasma. This happens if finally $T > T_c$ or a pressure $P(T) > P_B$ is reached before T exceeds T_c, a condition that may cause lattice failure and blister microexplosion. In this instance the whole phenomenon is accompanied by a neutron pulse, as is shown in more detail in Sec. VIII, where realistic n_0 values expected in CNF phenomena are discussed.

VIII. HYPERDENSITY IN BOSE-EINSTEIN-CONDENSED DEUTERIUM

Once n_0 reaches critical density n_{0_c}, i.e., the density where $T_c = T = T_0$ (initial real system temperature), then n_0, which does not appear in Eq. (25), continues to increase without affecting the pressure. The ultimate density levels depend on the efficiency of the deuteron discharge from the Pd metal lattice and on the feedback created by fusion-driven Bose-Einstein decondensation. According to Eqs. (33) and (24b), an efficient CNF system should reach sufficiently high n_0^{D} densities, higher than n_{0_c}, to achieve a density hysteresis, precluding a too-fast Bose-Einstein decondensation consequent to a fusion-driven temperature increase. After the maximum density n_M is reached (with corresponding maximum critical temperature $T_{MC} > T$), then, due to the energy released by fusions, plasma temperature T and pressure $P(T)$ will rise according to Eq. (25). The blisters and rifts often found enlarged in CNF cells result from $P(T)$ exceeding $P_B \cong 10^7$ bar before fusions terminate after a temperature $T > T_{MC}$ is reached. In other terms, once computed through Eq. (25), the temperature T_B at which $P = P_B$, the condition reached is

$$T_{MC} \geq T \geq T_{\mathrm{B}} \cong \left(\frac{10^7}{10^5}\right)^{2/5} \cdot T_0 = 10^{4/5} T_0 \cong 2000\ \mathrm{K}\ , \tag{34a}$$

which combined with Eq. (24b) leads to

$$\frac{n_M}{n_c} = \left(\frac{T_{MC}}{T_0}\right)^{3/2} \geq \left(\frac{T}{T_0}\right)^{3/2} \geq (10^{4/5})^{3/2} = 10^{6/5} \cong 16 \tag{34b}$$

and

$$n_0^{2/3} = \frac{T_0}{0.08 \cdot 10^{-17}}$$

$$n_c = n_0 = \left(\frac{3}{8}\, 10^{21}\right)^{3/2} \text{ deuterons/m}^3$$

$$\simeq 75 \times 10^{23} \text{ deuterons/cm}^3\ . \tag{34c}$$

Finally, Eqs. (34b) and (34c) combined show that when lattice failures are experimentally found, a maximum plasma density

$$n_M \geq 16 n_c \cong 16 \cdot 75 \cdot 10^{23} \text{ deuterons/cm}^3$$

$$\cong 1200 \times 10^{23} \text{ deuterons/cm}^3$$

is actually reached.

Hence the density in CNF phenomena, already of $75 \cdot 10^{23}$ at the beginning of BEC, often reaches values $> 10^3 \cdot 10^{23}$, i.e., $> 10^3$ times the solid densities. The neutronic optical size $\tilde{d} = d/\lambda = n_M \sigma_t^{\mathrm{D}n} d$ with d blister diameter and $\sigma_t^{\mathrm{D}n}$ total neutron-deuteron cross section can thus arrive at values $\tilde{d} \gg 1$, at least for the biggest hyperdense $\mathrm{D}_1^{2+} e^-$ zones or at least for a set of many hyperdense $\mathrm{D}_1^{2+} e^-$ zones.

This implies two main consequences: (a) the possibility to reach high RR_{FF}^{AB} for a time sufficient to heat plasma spots from 300 to 2000 K and (b) the possibility for hyperdense zones within a blister to trap neutrons and charged particles originating fusion chains.

Thus the annihilation of the Coulomb barrier predicted in Secs. V and VI alone explains the possibility of very high densities and fusion reaction rates, consistent heat generation, and fusion chains. In addition the behavior of these hyperdense zones as "supermetal zones," under BEC conditions, strongly damps any electromagnetic emission generated by the nuclear reactions inside the highly dense plasma spots itself.

Of course the realization of such eclatant phenomenology with the highest efficiency strongly depends on the optical thickness of plasma spots. Jones et al.'s[2] and similar experiments, showing relatively high neutron emission with undetectable energy generation, are probably due to insufficient values of blister density and of maximum plasma density n_M in the blisters. Efficient CNF systems, optically thick for neutrons, are characterized instead by low neutron emission compared with the energy release. The n and T_1^3 or p and He_2^3 multiplicative phenomena in hyperdense zones of $\mathrm{D}_1^{2+} e^-$ Bose-Einstein-condensed cold plasma are discussed in Sec. IX.

The dynamics of the creation and of the evolution of a single dense plasma zone and of the complete system resulting from their interactions will be the object of future investigations.

IX. NEUTRON AND T_1^3 MULTIPLICATION VIA D_1^2 DISINTEGRATION IN D-T AND D-He FUSION CHAINS INSIDE HYPERDENSE ZONES OF $\mathrm{D}_1^{2+} e^-$ BOSE-EINSTEIN-CONDENSED PLASMA

The D-D fusions are the main source of any other type of nuclear reaction. Eventual contributions of additional D-D-D fusions are ignored for simplicity.

The neutrons (n) or protons (p) emitted with energy of 2.4 MeV (n) and 3 MeV (p) during D-D fusions stay below the 3.3-MeV deuteron disintegration threshold and consequently slow down through pure elastic collisions. The $1/v$ absorption cross section for low-energy neutrons in D_1^{2+} associated with high $\tilde{d}$ implies that the majority of D-D fusion neutrons (or protons) will be completely thermalized and finally absorbed by D_1^2. The scheme of the reactions involved,

$$
\begin{array}{c}
\xleftarrow{\qquad 2(D_1^2 + D_1^2) \qquad}\\
\text{2 fusions}\\
\swarrow \qquad\qquad\qquad \searrow\\
T_1^{3+} + p + 4\ \text{MeV} \qquad\qquad He_2^3 + n + 3.2\ \text{MeV}\\
\downarrow \qquad\qquad\qquad \downarrow\\
D_1^2 + p \rightarrow He_2^3 + \gamma + 5.5\ \text{MeV} \qquad D_1^2 + n \rightarrow T_1^3 + \gamma + 6.2\ \text{MeV}\\
\hline
D_1^2 + D_1^2 + 2(D_1^2 + D_1^2) \rightarrow 2(T_1^3 + He_2^3 + \gamma) + 18.9\ \text{MeV}
\end{array} ,
$$

shows that any D-D fusion creates, directly or indirectly, one T_1^3 and one He_2^3 nucleus, which in turn, inside high-density $D_1^{2+}e^-$ regions, give rise to *n*-T-*n* and *p*-He-*p* chain loops as

n-T-*n* chain

$$
\begin{array}{c}
D_1^2 + T_1^3 \rightarrow He_2^4 + n + 17.6\ \text{MeV}\\
\uparrow \qquad \downarrow\\
\leftarrow D_1^2 + n \rightarrow T_1^3 + \gamma + 6.2\ \text{MeV}
\end{array}
$$

p-He-*p* chain

$$
\begin{array}{c}
D_1^2 + He_2^3 \rightarrow He_2^4 + p + 18.3\ \text{MeV}\\
\uparrow \qquad \downarrow\\
\leftarrow D_1^2 + p \rightarrow He_2^3 + \gamma + 5.5\ \text{MeV}
\end{array} .
$$

The elimination of the Coulomb barrier for fusions, when $T < T_{MC}$, makes RR_{FF} for D_1^{2+}-*p* of the same order of magnitude as the reaction rate for D_1^{2+}-*n*. The only evident difference between the neutron and proton slowing down is essentially the much shorter distance covered by the proton before absorption, which also implies much lower proton than neutron escapes from a hyperdense zone. The neutronic and protonic chains, cross-correlated through deuteron disintegrations $D(n,2n)p$ and $D(p,np)p$ generate additional neutrons and protons. The *p*-He-*p* is a strictly local multiplicative chain inside a single blister, whereas *n*-T-*n* is a collective multiplicative chain because neutrons generated inside a hyperdense plasma spot may go to interact with particles in another spot.

There are reactions collateral to the preceding main chains, typically neutron absorptions in He_2^3 or T-*p* fusions, responsible for reducing the number of neutrons and protons reacting with deuterium in the main chains and subtracting from them T_1^3 and He_2^3 ions.

Although the related cross sections are high, the number of reactions is limited due to the negligible concentrations of T_1^3 and He_2^3 in the $D_1^{2+}e^-$ plasma. Furthermore, the effect of cross multiplication via the interaction between the two chains should largely overcome the aforementioned reductive effects.

In fact, neutron multiplication via $D(n,2n)p$ in *n*-T-*n* chain yields protons to the *p*-He-*p* chain, and proton multiplication via $D(p,np)p$ in the *p*-He-*p* chain yields neutrons to the *n*-T-*n* chain, leading to $k_\infty - 1$ two times greater with respect to the value expected for each *n*-T-*n* or *p*-He-*p* chain considered in isolation.

The additional contribution to $k_\infty - 1$ of 6.2 and 5.5 MeV gammas due to *n*-D and *p*-D reactions is negligible. Once the He_2^4 nuclei are generated, secondary He_2^4-D_1^2 fusions generating Li_3^6 may also occur.

Other collateral effects are the enhancement of the fusion rates due to high-energy deuterons, resulting from elastic collisions with high-energy neutrons or positive ions generated by fusions, and the decreased multiplication introduced in the *p*-He-*p* chain by the continuous proton slowing down due to electromagnetic interactions with the surrounding plasma charges. These last three effects, disregarded for simplicity in the present work, are the aim of further calculations in progress. Since the two chains are symmetric with respect to $p \rightleftharpoons n$ exchange, we concentrate only on the *n*-T-*n* chain.

As shown in Ref. 6 and summarized in the Appendix, Monte Carlo and analytical treatments of the high-energy neutron slowing down by both elastic scattering and $D(n,2n)p$ disintegrations show a remarkable multiplication of neutrons *n* and T_1^3 in *n*-T-*n* chains. In fact, 14-MeV neutrons generated by D-T fusions and insufficiently slowed down, due to the high anisotropy of elastic scattering, exhibit such a high cross section for the $D(n,2n)p$ reaction that ~20% of the 14-MeV source neutrons directly disintegrate deuterium. The consideration of additional disintegrations, induced by scattered neutrons, together with second-order disintegrations, leads to the calculated value for multiplication factor of the *n*-T-*n* chain alone, $k_\infty = 1.4$ in the $D_1^{2+}e^-$ plasma Bose-Einstein-condensed. This result proves that for $\tilde{d} \gg 1$ or when a hyperdense "liquid" deuterium drops system of sufficient optical thickness fills the blisters, *n*-T-*n* chain reactions—and a fortiori *p*-He-*p* chain reactions—are possible, even when the effects on multiplication of the $D(\gamma,n)p$ reaction and of the interaction between the two chain loops are disregarded.

The neutron multiplication mechanism active during slowing down is illustrated in Fig. 1, where, for simplicity's sake, the multiple nonmultiplying elastic

Downloaded by [Australian Catholic University] at 05:53 21 September 2017

Downloaded by [Australian Catholic University] at 05:53 21 September 2017

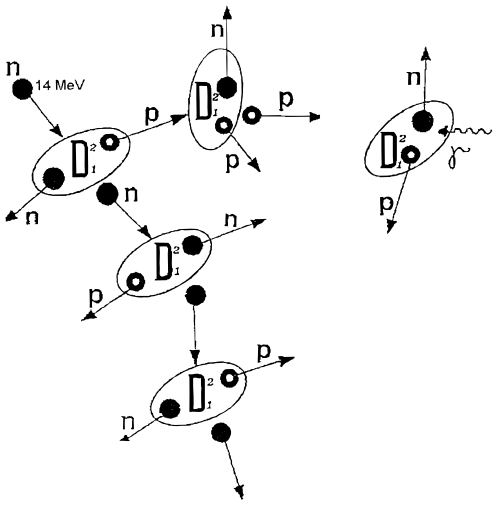

Fig. 1. Neutron multiplication via deuterium disintegrations.

collisions occurring between disintegrations have been omitted. Once thermalized inside hyperdense zones, the neutrons captured by D_1^2 nuclei generate an equal number of tritons. These tritons then diffuse at thermal energies up to when D-T fusions occur with associated emission of new 14-MeV neutrons. In this process, described in Fig. 2, any thermal neutron generates a triton in a way that k_∞ is identical for both T and *n*.

Lithium nuclei eventually present in hyperdense deuterium drops, as a product of triple D-D-D fusions or He_2^4-D fusions, contribute to T_1^3 multiplication and consequently to CNF phenomena, as indicated in the scheme of Fig. 3, reducing itself in pure deuterium drops (no Li) to the form with undotted lines only. Furthermore, since Li^+ is not expected to enter the metal lattice from outside, the presence of D-D-D or He_2^4-D fusions generating Li_3^6 should improve T_1^3 multiplication and so enhance CNF phenomena, whereas the substitution of Na for Li in the cell solution should nevertheless allow CNF, as experimentally verified by Appleby[3] and others.

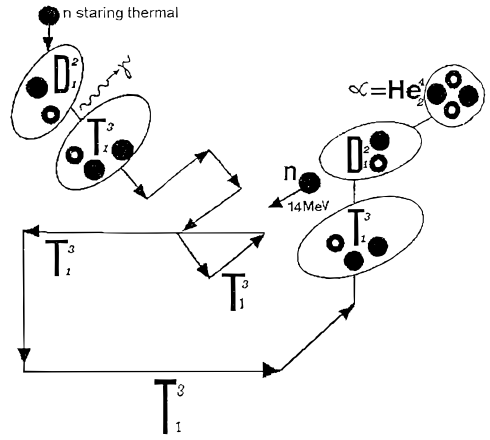

Fig. 2. The *n*-T-*n* chain kinetics.

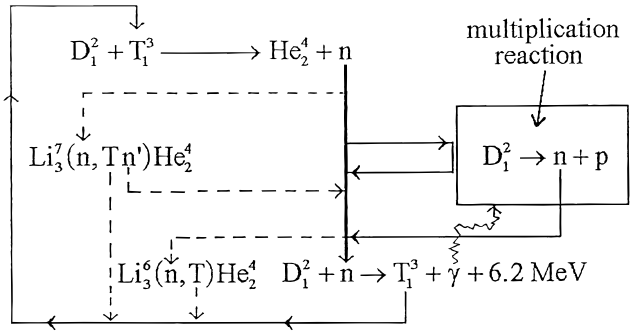

Fig. 3. The main two steps link.

The small fraction of neutrons escaping, after repeated collisions, from the hyperdense deuterium drops occupying the blister system implies an effective multiplication factor k_{eff} not so much less than k_∞. Although less optically thick CNF systems[28,39] exhibit a somewhat hard spectrum, more effective optically thick CNF systems will show a soft energy spectrum tail, suitable for $D_1^2(n,\gamma)T_1^3$ reactions in weakly dense deuterium zones inside Pd or in external D_2O solution. Thus only a few neutrons will escape from the entire CNF cell. Thence, though T_1^3 multiplies by $k_{eff} < k_\infty$ inside the hyperdense "liquid" deuterium drops system, T_1^3 will nevertheless multiply by $k_\infty \cong 1.4$ (or more due to cross multiplication of chains) in the physical system as a whole, with a continuous T_1^3 growth[3,40–43] during CNF phenomena. For extremely effective CNF cells, the spectrum of neutrons escaping from the hyperdense deuterium drops system could be so soft that practically all neutrons would be thermalized and quickly absorbed in heavily or weakly dense deuterium regions and in heavy water surrounding the Pd or Ti rod. This explains the excess heat and T_1^3 generation sometimes measured without neutron emissions, i.e., despite that the external neutron emission is of the order of the background. For these efficient CNF systems, the neutron chains of high k_{eff}, resulting from the relatively few neutron escapes from the multiple-blisters system, allow a collective behavior of the whole CNF system inside the metal. This collective neutronics causes a fortiori a proton chain high k_{eff}, with synergetic effects on the cross-correlated neutron chains. In weakly efficient CNF systems instead, proton multiplication could nevertheless take place inside isolated blisters, with only localized and correlated generation of neutron bursts.

X. TEMPERATURE AND PRESSURE EXCURSIONS CONSEQUENT TO FUSIONS

Inside any hyperdense deuterium drop, assumed to be initially composed of pure deuterium, the heat generated

Downloaded by [Australian Catholic University] at 05:53 21 September 2017

by D-D fusions, represented by a source S_Q, initially causes a low temperature distribution $t_0(\boldsymbol{x})$. The heat source S_Q is initially independent of D-T and D-He_2^3 fusion sources, being instead completely determined by the D-D fusion sources $S_{T_1^3}^{DD}[\boldsymbol{x}, t_0(\boldsymbol{x})]$ and $S_{He_2^3}^{DD}[\boldsymbol{x}, t_0(\boldsymbol{x})]$, associated with the direct or indirect production of T_1^3 and He_2^3 nuclei through D-D or *n*-D and *p*-D fusion reactions. If the condition $t_0(\boldsymbol{x}) < T_c$ is uniformly maintained through the drops, the fusion sources are independent of plasma temperature. The tritium and He^3 densities $n_{T_1^3}$ and $n_{He_2^3}$, as happens for neutron density in a fission reactor, will vary with time in accordance with the value of k_{eff}. The n_T and n_{He} densities will increase exponentially for $k_{eff} > 1$, linearly for $k_{eff} = 1$, and monotonically toward the asymptotic $n_{T_1^3}^{\infty} = S_{T_1^3}^{DD}[\boldsymbol{x}, t_0(\boldsymbol{x})]/(1 - k_{eff})$ and $n_{He_2^3}^{\infty}$ values until $k_{eff} < 1$ and the densities $n_{T_1^3}$ and $n_{He_2^3}$ remain at levels for which D-T and D-He_2^3 fusion heating cannot substantially affect plasma temperature.

The dependence of $n_{T_1^3}$ and $n_{He_2^3}$ on $(1 - k_{eff})$, when $0.95 < k_{eff} < 1$ causes a sensible increase in $n_{T_1^3}$ and $n_{He_2^3}$, correspondingly causing a rise in the D-T, D-He_2^3 fusion reaction rates and in the fusion heating in turn. Note that k_{eff} for a neutron chain and a proton chain may be different, due to weaker proton escapes from plasma spots. However, the local proton chain contributes to the neutron chain inside the same blister, whereas the neutron chain in a blister provides neutrons supporting proton chains locally active in other blisters. In other terms, neutron chains, locally less efficient than proton chains, have a global influence on the efficiency of the whole system.

During the D_1^2 discharge from the lattice into defects, the critical temperature T_c for the boson component of the plasma-filling blisters, due to Eq. (24b), increases with n_0 density through the following steps.

For an initial range of n_0 values starting from zero, T_c assumes values less than plasma temperature T initially equal to ambient temperature T_0. As n_0 approaches the value n_{0c}, critical for BEC at temperature $T = T_0$, the associated T_c nears $T = T_0$ and plasma approaches BEC. Once the n_{0c} density is reached, BEC begins and further increases of n_0 up to a maximum n_M, depending on the local CNF efficiency, lead T_c to a maximum critical temperature $T_{MC} > T_0$. Due to heat removal by the lattice, during the BEC process T remains at first approximately constant and so does the pressure $P(T) = P(T_c(n_{0_c})) = P(T_0) = 1.5 \times 10^5$ bar (for $T_0 = 300$ K). This continues up to the moment when the amount of heat generated by fusions, only partially removed, increases T above T_0 and so $P(T)$ above $P(T_0)$, according to Eq. (25). If P_B (P blistering) of the order of 10^7 bar represents the pressure required to modify the metal lattice surrounding the gap containing our Bose-Einstein-condensed plasma and T_B is the temperature such that $P(T_B) = P_B$, fusions will create different situations according to $T_{MC} > T_B$ or $T_{MC} < T_B$.

If $T_{MC} > T_B$, fusions, and thus temperature T and pressure P rise, will continue even when T exceeds T_B and consequently the pressure P exceeds P_B by starting a process of blister expansion within the lattice. Consequently, n_0 and T_c values decrease up to $T_c = T < T_{MC}$ and then to $T_c < T$ with the effect of gradual reappearance of the Coulomb barrier that inhibits the fusions. This behavior occurs in blisters of highly efficient CNF systems where n_M is as high as 10^3 solid density or more.

If $T_{MC} < T_B$, the increase of T and $P(T)$ should continue until the fusion reaction rates are attenuated because of T exceeding T_{MC}, but not T_B, so that $P(T)$ stays below P_B. In this instance the fusion phenomenon could cease or become steady state, leaving invariant the density at its maximum level during the whole fusion excursion, with no modification of the metal lattice structure.

XI. INTERPRETATION OF CNF PHENOMENOLOGY AND CONCLUSIONS

In this section we utilize the results obtained to explain the different CNF phenomenologies experimentally observed and to formulate the conclusions.

The last considerations in Sec. X directly explain the appearance, after 1 to 3 weeks, of blistering in palladium loaded with deuterium when the CNF phenomena occur efficiently, i.e., at high n_M density, when $T_{MC} > T_B$.

The second aspect of CNF phenomenology to discuss is related to the influence of the formation and dissolution of hyperdense zones in BEC on the neutronic k_{eff} and so on the CNF cell behavior.

The fast increases in fusion reaction rates RR_{FF}^{DD} or RR_{FF}^{DT} and RR_{FF}^{DHe} resulting from a sudden BEC in single blisters or from the increase in n_{He}, and the local generation of protons with cross-correlated neutron generation, represent fusion and neutron bursts. Such fusion bursts, involving, for $T_{MC} > T_B$, plasma and blisters macroexplosions, could be modeled via the equations of tritium and heat balances. These balances are connected via the source terms expressed by the energy released during the slowing down of fast particles and by D-D, D-T, and D-He fusion reaction rates corresponding to T_1^3 and He_2^3 generations, directly or via chain multiplication, with the k_{∞} factor. The dynamics will then depend on $P(T)$ relative to the temperature via Eq. (25). As already mentioned in Sec. VIII, this occurs for efficient CNF systems when Eq. (34a) holds so that finally T exceeds 2000 K, at least locally in a few blisters. For neutronic k_{eff} near 1 or greater than 1, the phenomenon will assume a collective character leading quickly to high temperatures throughout the metal.

If, after the initial charge of Pd via deuterium and consequent BEC, the multiplication k_{eff} factor for neutrons is <1, then the decrease of the neutron k_{eff} resulting from hyperdense zone explosions should prevent k_{eff} from exceeding 1. This fact suggests that a CNF system is intrinsically safe, provided that sudden increases in current density or sudden decreases in temperature T are not

induced from outside. In such a case additional discontinuous deuteron injections will increase the optical size of hyperdense zones and thus k_{eff}. This means that a sudden decrease in T or increase in current could lead the system to neutronically divergent hazardous conditions with a corresponding rapid increase in energy released from the system, as has been previously observed.

For cells where the k_{eff} decrease due to a single blister explosion is quickly counterbalanced by regular nucleation of new high-density BEC deuterium zones, the bursts merge into a continuous neutron and heat emission. However, for less-efficient cells, the burst will remain isolated. When isolated bursts may simply follow from BEC and D-D fusions with associated proton chain generation, a collective CNF phenomenon involving the whole system is necessarily related to an *n*-T-*n* neutron fusion chain and correlated phenomena, if no protons are injected from the outside.

In gaseous CNF, the low temperature reached in cooling, followed by temperature increase, enhances the creation of $D_1^{2+}e^-$ plasma Bose-Einstein-condensed zones, whereas resulting higher temperatures cannot dissolve these zones before a few neutron and fusion bursts could occur, eventually enhanced by the aggregation or enlargement of BEC zones induced just by the T increase with D_1^{2+} expulsions from the lattice.

The third aspect of CNF phenomenology to be interpreted is the interaction of a CNF cell with an external, involving neutron chain, gamma emission and superconductivity, and the CNF dependence on the density of voids inside the cell, seen before in view of reactions of the cell to external actions and then as the possibility of controlling the CNF cell.

Within the framework of the CNF theory proposed here, experimentally observed neutron spectra exhibiting remarkably wide peaks at energies higher than 2.4 MeV, e.g., from 3 to 14 MeV (see, for example, Refs. 39 and 44), can be interpreted as due to 14-MeV D-T fusion neutrons, slowed down by elastic collisions and deuteron $D(n,2n)p$ disintegrations inside an optically thin (not effective) hyperdense Bose-Einstein-condensed $D_1^{2+}e^-$ plasma drops system and escaping from them after a few interactions. The CNF sensitivity to neutron background[45] and the possibility of CNF induction by external neutron injection[19] are obvious consequences of considering neutrons as chain carriers in *n*-T-*n* fusion chains. This fact indicates a clear way to control and enhance CNF via neutronics. Future experiments should be planned to measure T_1^3 space distributions outside Pd to deduce the neutron emission spectrum from the cathode of a CNF cell and determine total T_1^3 generation, further detecting neutron emissions with appropriate diagnostics.

The hysteresis in the coupling of the BEC initial phenomenon and the fusion-driven temperature rise with related blister microexplosions indicates that CNF phenomena may be controlled by varying the size and density distribution of voids. An optimal void density in metal could then be identified and achieved as follows.

Since the equilibrium concentration of voids varies with temperature according to the $n_v = e^{-E_v/kT}$ law, a fast temperature decrease from a high T equilibrium state will freeze in the lattice the level of defects required. Once n_v is known, cell calculation techniques, currently used for fission reactors, could be applied to compute k_∞ and k_{eff} for neutron multiplication in a hydrogenized metal lattice of blisters filled with hyperdense $D_1^{2+}e^-$ Bose-Einstein-condensed plasma. Monte Carlo or stochastic calculations could eventually be adopted for complicated blister shapes.

A strong suppression of electromagnetic emissions from inside the Bose-Einstein-condensed plasma results from Coulomb barrier annihilation by BEC with associated high densities and supermetallic behavior. Emissions of electromagnetic radiation could occur during the initial BEC or the final Bose-Einstein-decondensation period of a hyperdense single zone, creating cold surface sources in the first case and much warmer ones in the second.

Of course the strong tritium multiplication inside the whole system as well as low neutron emission depend on the high D_1^2 density reached in initial BEC.

Also, collateral superconductivity effects, better for D_1^2 than for H_1^1, can be justified on the basis of the electrical behavior of the $D_1^{2+}e^-$ BEC plasma.

The CNF sensitivity to the T_1^3 percentage in D_2O, to the neutron background, to the concentration of Be^9 and of other neutron multipliers, such as Pb, and finally to the density of defects in the lattice should be essentially tested and then used in view of CNF control. Neutron multipliers or tritiogenic materials, such as Li_3^6, could also be incorporated in metals through ion implantation and high-temperature diffusion techniques or insertion of regular heterogeneous zones into the metal by standard techniques.

The present theory confined itself to explain the main CNF phenomenologies to provide a few indications to researchers. The given description of CNF systems points up the need for new and more profound studies, in view of their optimization and control, in the special following areas:

1. time-dependent nonequilibrium study of the BEC process
2. evolution of hyperdense zones during fusion-driven heating and successive RR_{FF} attenuation via Coulomb barrier reappearance as T exceeds T_{MC}
3. detailed evolution of fusion chains and collateral nuclear reactions in CNF systems made by multiple blisters filled with Bose-Einstein-condensed D_1^2 plasma
4. neutron, proton, and gamma-ray cross-combined transport processes.

Downloaded by [Australian Catholic University] at 05:53 21 September 2017

These unexplored fields of research call for a new appropriately developed mathematical physics and for the associated calculational algorithms, which are to some extent already in progress.[46,47]

A last indication of the proposed qualitative theoretical approach to CNF is that CNF phenomena could be obtained even outside metal lattices, provided a sufficiently high containment pressure P is suddenly applied to a sufficiently cold ionized deuterium whose temperature T, correlated to P by Eq. (25), is much less than $T_0 = 300$ K; once BEC occurs, temperature can be allowed to increase, as in the D'Amato et al.[18] experiment, due to density hysteresis, as previously illustrated. An initial efficient cooling system should not only lead deuterium to $T \ll T_0$ temperature (near absolute zero to reduce the containment pressure required) but should also remove the heat released by Bose-Einstein-condensing plasma. According to Ref. 48, a facility to test the predicted results could be composed of a diamond anvil cell[49–51] irradiated by a suitable X-ray source.

APPENDIX

HIGH-ENERGY NEUTRON MULTIPLICATION VIA D(n,2n)p REACTION DURING SLOWING DOWN IN DEUTERIUM

Until now, neutron-induced deuterium disintegrations were disregarded in neutron slowing-down treatments because the 3.3-MeV threshold energy for such reactions is higher than the energies usually exhibited by most neutrons in fission reactors. But, appropriate modeling of CNF phenomena and hot fusion T_1^3 generation in D_2O blankets demands an accurate consideration of the D$(n,2n)p$ reaction effects on neutron slowing down. The Monte Carlo simulation of such effects requires a detailed knowledge of the energy-angle transference function for such reactions. Analogous to the kinematics of neutron-nucleus inelastic scattering, classical conservation laws in the D$(n,2n)p$ reaction yield

$$E_{n_1} = E'_{n_1}[1/(A+1)^2][A^2R^2_{n_1}(E'_{n_1},\beta,\beta^{(C)}) + 2AR_{n_1}(E'_{n_1},\beta,\beta^{(C)})\cos\vartheta_1 + 1] \ ,$$

$$E_p = E'_{n_1}[1/(A+1)^2][A^2R^2_{p}(E'_{n_1},\beta,\beta^{(C)}) + 2AR_{p}(E'_{n_1},\beta,\beta^{(C)})\cos\vartheta_p + 1] \ ,$$

and

$$E_{n_2} = E'_{n_1}[1/(A+1)^2][A^2R^2_{n_2}(E'_{n_1},\beta,\beta^{(C)}) + 2AR_{n_2}(E'_{n_1},\beta,\beta^{(C)})\cos\vartheta_2 + 1]$$

for the energy of the outgoing particles in terms of the original energy En_1 of the neutron inducing the reaction, through $A = 2$ for the deuteron,

$$R_{n_1}(E'_{n_1},\beta,\beta^{(C)}) = \left\{ \frac{1 - \dfrac{A+1}{A}\dfrac{E_D}{E'_{n_1}}}{2\dfrac{A}{A+1}x^2(\beta,\beta^{(C)}) + 1} \right\}^{1/2} \quad , \quad \text{with } E_D = 2.2 \text{ MeV}$$

and

$$x = \frac{\cos\beta[1-\cos^2\beta^{(C)}] + |\cos\beta^{(C)}|\,\{[1-\cos^2\beta^{(C)}][1-\cos^2\beta]\}^{1/2}}{2[\cos^2\beta^{(C)} - \cos^2\beta]} \ ,$$

$$R_p(E'_{n_1},\beta,\beta^{(C)}) = (x^2 + x\cos\beta + \tfrac{1}{4})^{1/2}R_{n_1}(E'_{n_1},\beta,\beta^{(C)}) \ ,$$

and

$$R_{n_2}(E'_{n_1},\beta,\beta^{(C)}) = (x^2 - x\cos\beta + \tfrac{1}{4})^{1/2}R_{n_1}(E'_{n_1},\beta,\beta^{(C)})$$

with angles defined as in Fig. A.1.

Downloaded by [Australian Catholic University] at 05:53 21 September 2017

Downloaded by [Australian Catholic University] at 05:53 21 September 2017

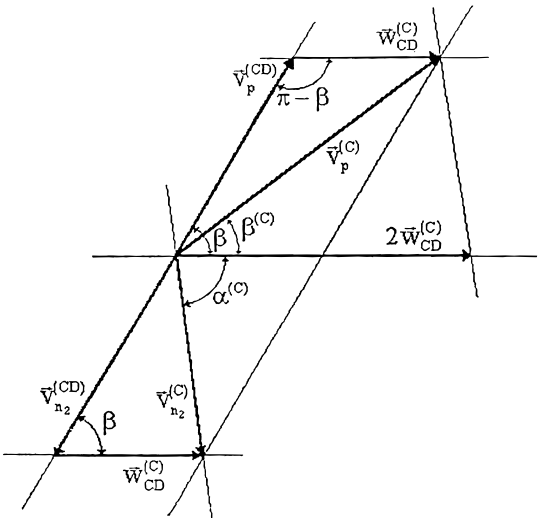

Fig. A.1. Deuterium disintegration seen from its c.m. system CD.

From the R_{n1} definition follows a threshold energy

$$E_{n_1}^{th} = \frac{A+1}{A} E_D = \frac{3}{2} \cdot 2.2 \text{ MeV} = 3.3 \text{ MeV} \ ,$$

as the minimum energy of the incident neutron allowing deuteron disintegration without violation of energy and momentum conservation laws.

The cosines of the angles between the incident neutron velocity and the velocities of the three outgoing particles with respect to the laboratory reference system $\cos \vartheta_1^L$, $\cos \vartheta_2^L$, $\cos {}_p^L$ are then expressed in terms of the corresponding cosines $\cos \vartheta_1$, $\cos \vartheta_2$, $\cos \vartheta_p$ with respect to the three particles center-of-mass (c.m.) reference system as

$$\mu_{12p}^L = \frac{AR_{n_1 n_2 p}(E'_{n_1}, \beta, \beta^{(C)}) \mu_{12p} + 1}{A^2 R_{n_1 n_2 p}^2(E'_{n_1}, \beta, \beta^{(C)}) + 2AR_{n_1 n_2 p}(E'_{n_1}, \beta, \beta^{(C)}) \mu_{12p} + 1}$$

with

$$\mu_{12p} = \cos \vartheta_{12p} \ , \quad \mu_{12p}^L = \cos \vartheta_{12p}^L \ .$$

The Monte Carlo model simulating 14-MeV neutron slowing down in deuterium adopts standard techniques for elastic scattering and combines the preceding D$(n,2n)p$ kinematic results with the usual randomization for emitted neutrons and protons. The main problem for Monte Carlo simulation is that posed by the bifurcation of neutron histories implied by the D$(n,2n)p$ reaction. After any disintegration, the history of the n_1 neutron is further followed, whereas position, energy, and direction of the n_2 neutron are stored one by one; the corresponding proton data are also stored in view of future proton transport calculations.[47]

Every time that for a specific neutron En_1 becomes less than $E_{cutoff} = 1$ eV, the computation restarts from the initial data stored, following another history for an n_2 neutron.

The calculation performed within the framework of a 30-energy-group scheme allows one to obtain the energy spectrum of escaping neutrons, the space distribution of the thermalized neutrons within the cylindrical geometry adopted, and the multiplication factor

$$k = \frac{\text{neutrons thermalized inside the system}}{\text{fast neutrons generated by the 14-MeV source}} \cong k_\infty$$

for an optically wide system. For cross control with Monte Carlo results on k_∞, an analytical spectral calculation for an infinite system has been performed on the basis of the equation

$$\Sigma(E)\varphi(E) = \delta(E - E_0) + \int_E^{E/\alpha} \Pi_{e1}(E' \to E)\Sigma(E')\varphi(E')\, dE' + \int_{f_{1d}(E)}^{f_{2d}(E)} \Pi_d(E' \to E)\Sigma_d(E')\varphi(E')\, dE' \ .$$

In terms of the fluxes $\phi_n(E)$ of the neutrons passed through n disintegrations and disregarding $\phi_n(E)$ for $n \geq 1$, k_∞ is finally expressed as

$$k_\infty = 1 + \int_{E_{thd}}^{E_0} \Sigma_d(E')\phi_0(E')\, dE'$$

through the solution $\phi_0(E)$ of the equation

$$\Sigma(E)\phi_0(E) = \delta(E - E_0) + \int_E^{E/\alpha} \Pi_{e1}(E' \to E)\Sigma_s(E')\phi_0(E')\, dE'$$

with $\Sigma(E) = \Sigma_s(E) + \Sigma_d(E)$ and $\alpha = (A-1)^2/(A+1)^2 = \frac{1}{9}$ for deuterium, $\Sigma_d(E)$ being the disintegration cross section for a neutron.

With the separation of $\phi_0(E)$ into the sum of virgin flux $\delta(E - E_0)/\Sigma(E)$ and collided flux $\phi_{0c}(E)$ once defined the collision density $F(E) = \Sigma(E)\ \phi_{0c}(E)$ and

$$h(E) = \frac{\Sigma_s(E)}{\Sigma(E)} = 1 - \frac{\Sigma_d(E)}{\Sigma(E)} \ ,$$

the solution of the equation

$$F(E) = \frac{1}{1-\alpha} \int_E^{E_0} h(E')F(E') \frac{dE'}{E'} + \frac{h(E_0)}{(1-\alpha)E_0}$$

in the group discretization scheme assumes the recurrent character

$$F_g = \left(\frac{E_{g-1}}{E_g} \right)^{\alpha_g} F_{g-1} \quad \text{with} \quad \alpha_g = \frac{h_g}{1-\alpha} \ ,$$

expressing in a discretized form the "continuous recursivity" of the Volterra integral equation for $F(E)$. This finally leads to the recurrent algorithm

$$q_0 = 1 \qquad q_g = q_{g-1} - [1 - h_g]\delta_g$$

with

$$\delta_g = \frac{1}{1 - \alpha_g}\left[E_{g-1}F_{g-1} - E_g F_g\right]$$

and

$$k_\infty = 2 - q_9 \qquad [\text{as } q(E_{thd}) = (q_g)_{g=9} = 2 - k_\infty] \ ,$$

finally allowing the estimation of k_∞.

The numerical results obtained for k_∞ are the following:

	Analytical	Monte Carlo
1. isotropic scattering with one disintegration	$k_\infty = 1.29$	1.29
2. isotropic scattering with any number of disintegrations	$k_\infty =$	1.33
3. anisotropic scattering with any number of disintegrations and extrapolated results	$k_\infty =$	1.40
4. for neutron contribution due to $D(p,np)p$	$k_\infty \approx 1.80$	
5. for neutron contribution due to $D(\gamma,n)p$	$k_\infty = 1.82$	

Finally, Monte Carlo simulation of the transport of neutrons generated by a 14-MeV source inside a small high-density cylinder immersed in a deuterated cell, representing a realistic system, confirms that only a few strongly slowed down neutrons can escape outside the CNF cell.

ACKNOWLEDGMENTS

Enlightening discussions with E. Cupini, P. Cammarota, C. Stremmenos, S. De Pasca, and G. Luca Luigi are gratefully acknowledged as well as their Monte Carlo calculation of neutron k_∞ in deuterium, suggestions resulting from experimental considerations, ideas on boson transport, and selective collection of quantum transport documents. The contributions of C. Elliott and M. Vallicelli to the final English version of the paper are also gratefully acknowledged.

REFERENCES

1. M. FLEISCHMANN and S. J. PONS, "Electrochemically Induced Nuclear Fusion of Deuterium," *J. Electroanal. Chem.*, **261**, 301 (1989).

2. S. E. JONES et al., "Observation of Cold Nuclear Fusion in Condensed Matter," *Nature*, **338**, 737 (1989).

3. A. J. APPLEBY, "Evidence for Excess Heat Generation Rates During Electrolysis of D_2O in LiOD Using a Palladium Cathode-A Microcalorimetric Study," presented at Workshop on Cold Fusion Phenomena, May 23–25, 1989, Santa Fe, New Mexico.

4. F. PREMUDA, *Sci. Corresp. Nature*, **238**, 712 (Apr. 27, 1989).

5. F. PREMUDA, "Fusion Chain Reactions in Fleischmann and Pons Experiment," LIN Report 0901 (1989).

6. F. PREMUDA, "Multiplication of High Energy Neutrons in a Deuterium Plasma," presented at ICIAM 91, Washington, D.C., July 8–12, 1991 (see Abstracts, p. 169).

7. M. VASELLI, M. HARITH, V. PALLESCHI, G. SALVETTI, and D. P. SINGH, "Screening Effect of Impurities in Metals: A Possible Explanation of the Process of Cold Nuclear Fusion," *Nuovo Cimento*, **11D**, *6*, 927 (June 1989).

8. T. BRESSANI, E. DEL GIUDICE, and G. PREPARATA, "First Steps Towards an Understanding of Cold Nuclear Fusion," *Nuovo Cimento*, **101A**, *5*, 845 (May 1989).

9. G. PREPARATA, "Some Theories of 'Cold' Nuclear Fusion: A Review," *Fusion Technol.*, **20**, 82 (1991).

10. H. HORA, J. C. KELLY, J. U. PATEL, M. A. PRELAS, J. H. MILEY, and J. W. TOMPKINS, "Screening in Cold Fusion Derived from D-D Reactions," *Phys. Lett.*, **A175**, 138 (1993).

11. Y. E. KIM, "Surface Reaction Mechanism for Deuterium-Deuterium Fusion with a Gas/Solid-State Fusion Device," *Fusion Technol.*, **19**, 558 (1991).

12. R. A. RICE, G. S. CHULICK, Y. E. KIM, and J.-H. YOON, "The Role of Velocity Distribution in Cold Deuterium-Deuterium Fusion," *Fusion Technol.*, **18**, 147 (1990).

13. G. E. UHLENBECK and L. GROPER, "The Equation of State of a Non-Ideal Einstein-Bose or Fermi-Dirac Gas," *Phys. Rev.*, **41**, 79 (1932).

14. A. ISIHARA and M. WADATI, "Screening Constants for Systems of Charged Particles," *Phys. Rev.*, **183**, 312 (1969).

15. R. BALESCU, *Equilibrium and Nonequilibrium Statistical Mechanics*, Krieger Publishing Company, Huntington, New York (1991).

16. G. PREPARATA, "Cold Fusion: What Do the Laws of Nature Allow and Forbid?" *Proc. 2nd Annual Conf. Cold Fusion, Italian Physical Society Conference Proceedings*, Vol. 33, p. 453 (1991).

17. S. N. VAIDYA, "Comments on the Model for Coherent Deuteron-Deuteron Fusion in Crystalline Pd-D Lattice," *Fusion Technol.*, **24**, 112 (1993).

18. J. D'AMATO, A. DE NINNO, F. SCARAMUZZI, P. ZEPPA, C. PINTORIERI, and F. LANZA, "Search for Nuclear Phenomena by the Interaction Between Titanium and Deuterium," presented at 1st Annual Conf. Cold Fusion, Salt Lake City, Utah, March 28–31, 1990.

19. F. CELANI et al., "Search for Neutron Emission from Deuterided High Temperature Superconductors in Very Low Background Environment," *Proc. 2nd Annual Conf. Cold Fusion, Italian Physical Society Conference Proceedings*, Vol. 33, p. 113 (1991).

Downloaded by [Australian Catholic University] at 05:53 21 September 2017

Downloaded by [Australian Catholic University] at 05:53 21 September 2017

20. F. LANZA, G. BERTOLINI, V. VOCINO, E. PARNISARI, and C. RONSECCO, "Tritium Production Resulting from Deuteration of Different Metals and Alloys," *Proc. 2nd Annual Conf. Cold Fusion, Italian Physical Society Conference Proceedings*, Vol. 33 (1991).

21. W.-X. ZHANG, "Possibility of Phase Transitions Inducing Cold Fusion in Palladium/Deuterium Systems," *Fusion Technol.*, **21**, 82 (1992).

22. L. H. BAGNULO, "Crack-Fusion: A Plausible Explanation of Cold Fusion," *Proc. 2nd Annual Conf. Cold Fusion*, Italian Physical Society Conference Proceedings, Vol. 33 (1991).

23. R. L. LIBOFF, "Fusion via Metallic Deuterium," *Phys. Lett.*, **71A**, *4*, 361 (1979).

24. R. L. LIBOFF, "Fusion Through Metallic Deuterium. Part II," *Phys. Lett.*, **74A**, *5*, 323 (1979).

25. D. K. LEE and E. FEENBERG, "Ground State and Low Excited States of a Boson Liquid with Applications to the Charged Boson System," *Phys. Rev.*, **137**, *A3*, 731 (1965).

26. J. P. HANSEN and R. MAZIGHI, "Ground State of the Strongly Coupled Charged Bose Gas," *Phys. Rev.*, **18**, *A3*, 1282 (1978).

27. L. C. CASE, "The Reality of 'Cold Fusion,' " *Fusion Technol.*, **20**, 478 (1991).

28. A. TAKAHASHI, "Nuclear Products by D_2O/Pd Electrolysis and Multibody Fusion," presented at ISEM, Nagoya, Japan, January 27, 1992.

29. J. DUFOUR, "Cold Fusion by Sparking in Hydrogen Isotopes," *Fusion Technol.*, **24**, 205 (1993).

30. R. MORE, "Atoms in Plasmas," *Phys. World*, *4*, 38 (Apr. 1992).

31. W. D. KRAEFT and D. KREMP, "Nonideal Plasma and Bound States," *Strongly Coupled Plasma Physics*, NATO ASI Series B, Vol. 154, p. 199, F. J. ROGERS and H. E. DEWITT, Eds., Plenum, New York.

32. R. L. LIBOFF, *Kinetic Theory, Classical, Quantum, and Relativistic Descriptions*, Prentice Hall (1989).

33. E. A. UEHLING and G. E. UHLENBECK, "Transport Phenomena in Einstein-Bose and Fermi-Dirac Gases I," *Phys. Rev.*, **43**, 552 (1933).

34. F. PREMUDA, "Bosonic Transport via Boltzmann-Uehling-Uhlenbeck Equation at Subcritical Temperatures" summary sent to the Secretariat of GNFM of the CNR (National Research Council) (May 27, 1993) (in Italian).

35. G. LUIGI, "Transport Process in Cold Plasmas in the Light of Quantum Kinetic Foundations," Thesis, Bologna University (July 1993) (in Italian).

36. M. N. ROSENBLUTH and R. Z. SAGDEEV, *Handbook of Plasma Physics; Vol. I Basic Plasma Physics 1*, North Holland, Amsterdam (1983).

37. F. PREMUDA, R. SANTUCCI, and S. STANGHELLINI, "Thomas-Fermi Equation for Inter-Deuteron Potential Screening in a Degenerate Deuterium Plasma" (to be published).

38. E. SEGRÈ, "Nuclei e particelle," Zanichelli Bologna (1966).

39. A. TAKAHASHI, T. IIDA, T. TAKEUCHI, A. MEGA, S. YOSHIDA, and M. WATANABE, "Neutron Spectra and Controllability by Pd/Electrolysis Cell with Low-High Current Pulse Operation," *Proc. 2nd Annual Conf. Cold Fusion, Italian Physical Society Conference Proceedings*, Vol. 33, p. 93 (1991).

40. P. K. IYENGAR and M. SRINIVASAN, "Overview of BARC Studies in Cold Fusion," presented at 1st Annual Conf. Cold Fusion," Salt Lake City, Utah, March 28–31, 1990.

41. M. S. KRISHNAN et al., *Fusion Technol.*, **18**, 35 (1990).

42. M. S. NAYAR et al., *Fusion Technol.*, **18**, 39 (1990).

43. T. S. MURTHY, T. S. IYENGAR, B. K. SEN, and T. B. JOSEPH, *Fusion Technol.*, **18**, 71 (1990).

44. V. D. RUSOV, T. N. ZELENTSOVA, M. Y. SEMENOV, I. V. RADIN, Y. F. BABIKOVA, and Y. A. KURGLYAK, *Pris'ma Zh. Tekh. Fiz.*, **15** (1989) (in Russian).

45. S. SAHNI, C. COHEN, A. GRAYEVSKY, and A. BROKNAN, "Evidence for a Background Neutron Enhanced Fusion in Deuterium Absorbed Palladium," *Solid State Commun.*, **72**, 53 (1989).

46. V. D. LEVCHENKO, F. PREMUDA, and Y. S. SIGOV, "1/2 D Numerical Simulation of Nonideal Vlasov-KBG Plasma Using Splitting Technique," *Proc. SIMAI '94*, Anacapri, Italy, May 31–June 3, 1994 (1994).

47. L. PETRIZZI, "A Monte Carlo Treatment of Combined High Energy Neutron and Proton Slowing-Down in Deuterium," PhD Thesis, Bologna University.

48. C. STREMMENOS, Private Communication.

49. W. A. WILDHAC, "Proton Deuteron Transformation as a Source of Energy in Dense Stars," *Phys. Rev.*, **57**, 81 (1940).

50. G. V. FEDOROVICH, "A Possible Way to Nuclear Fusion in Solids," *Fusion Technol.*, **24**, 288 (1993).

51. A. JAYARAMAN, "Recent Developments in Static High Pressure Research," *Rev. Mod. Phys.*, **55**, 65 (1983).

Francesco Premuda (Dr., physics, Università degli Studi di Trieste, Italy, 1962) is currently associate professor of nuclear advanced reactors in the Nuclear Engineering Laboratory of Montecuccolino, section of DIENCA Department of the Engineering Faculty of Bologna University. His present primary research interests include anisotropic neutron transport in fission reactors; charged-particle transport in inertial confinement fusion reactors; Monte Carlo and deterministic multiplicative neutron and proton slowing down in deuterium, kinetics, and electrodynamics of degenerate plasmas; and superconductive effects in cold degenerate plasmas.